Effects of Frozen Soil on Soil Temperature, Spring Infiltration, and Runoff: Results from the PILPS 2(d) Experiment at Valdai, Russia

Lifeng Luo,[a] Alan Robock,[a] Konstantin Y. Vinnikov,[b] C. Adam Schlosser,[c] Andrew G. Slater,[d] Aaron Boone,[e] Harald Braden,[f] Peter Cox,[g] Patricia de Rosnay,[h] Robert E. Dickinson,[i] Yongjiu Dai,[j] Qingyun Duan,[k] Pierre Etchevers,[e] Ann Henderson-Sellers,[l] Nicola Gedney,[m,*] Yevgeniy M. Gusev,[n] Florence Habets,[e] Jinwon Kim,[o] Eva Kowalczyk,[p] Kenneth Mitchell,[q] Olga N. Nasonova,[n] Joel Noilhan,[e] Andrew J. Pitman,[r] John Schaake,[k] Andrey B. Shmakin,[s] Tatiana G. Smirnova,[t] Peter Wetzel,[u] Yongkang Xue,[v] Zong-Liang Yang[w], and Qing-Cun Zeng[j]

[a] *Department of Environmental Sciences, Rutgers University, New Brunswick, NJ, USA*
[b] *Department of Meteorology, University of Maryland, College Park, MD, USA*
[c] *Goddard Earth Sciences and Technology Center, NASA/GSFC, Greenbelt, MD, USA*
[d] *CIRES, University of Colorado, Boulder, CO, USA*
[e] *Météo-France/CNRM, Toulouse, France*
[f] *Agrometeorologic Research, German Weather Service, Braunschweig, Germany*
[g] *Hadley Centre for Climate Prediction and Research, Bracknell, Berkshire, UK*
[h] *Laboratoire de Meteorologie Dynamique du CNRS, Paris, France*
[i] *School of Earth and Atmospheric Sciences, Georgia Institute of Technology, Atlanta, GA, USA*
[j] *Institute of Atmospheric Physics, Chinese Academy of Sciences, Beijing, China*
[k] *Office of Hydrology, NOAA, Silver Spring, MD, USA*
[l] *Australian Nuclear Science and Technology Organisation, Sydney, Australia*
[m] *Meteorology Department, Reading University, UK*
[n] *Institute of Water Problems, Moscow, Russia*
[o] *Department of Atmospheric Sciences, University of California Los Angeles, Los Angeles, CA, USA'*
[p] *Division of Atmospheric Research, CSIRO, Aspendale, Australia*
[q] *Environmental Modeling Center, NOAA/NCEP, Camp Springs, MD, USA*
[r] *Department of Physical Geography, Macquarie University, Sydney, Australia*
[s] *Institute of Geography, Moscow, Russia*
[t] *Forecast Systems Laboratory, NOAA, Boulder, CO, USA*
[u] *Mesoscale Dynamics and Precipitation Branch, NASA/GSFC, Greenbelt, MD, USA*
[v] *Department of Geography, University of California Los Angeles, Los Angeles, CA, USA*
[w] *Department of Geological Sciences, University of Texas, Austin, TX, USA*
* *Now at Hadley Centre for Climate Prediction and Research, Bracknell, Berkshire, UK*

Submitted to *Journal of Hydrometeorology*

June, 2002

Revised October, 2002

Corresponding Author:
Alan Robock
Department of Environmental Sciences
Rutgers University
14 College Farm Road
New Brunswick, NJ 08901-8551
Phone: 732-932-9478
Fax: 732-932-8644
Email: robock@envsci.rutgers.edu

Abstract

The Project for Intercomparison of Land-surface Parameterization Schemes Phase 2(d) experiment at Valdai, Russia, offers a unique opportunity to evaluate land surface schemes, especially snow and frozen soil parameterizations. Here we examine the ability of the 21 schemes that participated in the experiment to correctly simulate the thermal and hydrological properties of the soil on several different time scales. Using observed vertical profiles of soil temperature and soil moisture, we evaluate the impact of frozen soil schemes in the land surface models on the soil temperature and soil moisture simulations.

We find that when soil-water freezing is explicitly included in a model, it improves the simulation of soil temperature and its variability at seasonal and interannual scales. Although change of thermal conductivity of the soil also affects soil temperature simulation, this effect is rather weak. The impact of frozen soil on soil moisture is inconclusive in this experiment due to the particular climate at Valdai, where the top 1 m of soil is very close to saturation during winter and the range for soil moisture changes at the time of snowmelt is very limited. The results also imply that inclusion of explicit snow processes in the models would contribute to substantially improved simulations. More sophisticated snow models based on snow physics tend produce better snow simulations, especially of snow ablation. Hysteresis of snow cover fraction as a function of snow depth is observed at the catchment but not in any of the models.

1. Introduction

The land surface is an important component of the climate and weather system. The numerical expression of land surface processes plays an important role in both climate and weather forecast models (e.g., Henderson-Sellers et al. 1993, Gedney et al. 2000). As part of the lower boundary of the atmosphere, the land surface is strongly connected with atmospheric variations in several ways. By affecting water and energy flows between the land surface and the atmosphere, the thermal and hydrological status of the soil is strongly connected with the atmosphere. A large number of land surface schemes (LSSs) have been designed to simulate land surface processes in a variety of numerical ways. Models include all the important processes but might emphasize different ones depending on their specific goals.

The Project for Intercomparison of Land-surface Parameterization Schemes (PILPS) aims to improve understanding of the parameterization of interactions between the atmosphere and the continental surface in climate and weather forecast models (Henderson-Sellers et al. 1993, 1995). PILPS Phase 2(d) (Schlosser et al., 2001) was designed to investigate land surface simulations in a climate with snow and seasonally frozen soil, making use of a set of meteorological and hydrological data spanning 18 years (1966-1983) from a grassland catchment at the Valdai water-balance research station in Russia (Vinnikov et al. 1996, Schlosser et al. 1997). This off-line experiment uses meteorological and radiation data as forcing and hydrological data to evaluate the LSS performances. A pilot study (Schlosser et al. 1997) using two LSSs, a simple bucket hydrology model (Budyko 1956, Manabe 1969) and a more complex biosphere model (SSiB; Xue et al. 1991), illustrated the suitability of these data sets for stand-alone simulations.

There are several advantages in the PILPS 2(d) experiment compared with other PILPS Phase 2 experiments. The seasonal snow cover at Valdai allows us to evaluate snow schemes in the participant LSSs, examining both seasonal cycles and interannual variations. Seasonally frozen soil also offers a unique opportunity to check the model simulations of soil temperature

and the frozen soil schemes, if present. (When the soil temperature is below 0°C, it is the water in the soil that is frozen. Therefore, whenever we use the term "frozen soil" we really mean "frozen soil water.") Since runoff simulation is affected both by snow and the partitioning of meltwater in the models, the role of the frozen soil physics in the partitioning of meltwater can be evaluated based on daily observations of runoff and soil temperatures. Additionally, the Valdai experiment runs for 18 years, allowing both the seasonal cycle and interannual variations to be investigated.

21 LSSs (Table 1), of varying complexity and based on different modeling philosophies, participated in PILPS 2(d). They performed a control simulation and five additional simulations designed to address the sensitivity of the LSSs to downward longwave radiation forcing, and the timescale and causes of simulated hydrological variability (Schlosser et al. 2000). Schlosser et al. (2000) focused on the hydrological outputs of model simulations requested by PILPS 2(d) and compared the models' performance against observed data on seasonal and annual time scales. They concluded that the models' root-zone soil moisture falls within the observed spatial variability in nearly all cases, which indicates that models can capture the broad features of soil moisture variations. They analyzed the water-flux partition on an annual basis and found that nearly all the models partition the incoming precipitation into evaporation and runoff in a manner similar to observations in a broad sense. But they also pointed out that there is quite a bit of inter-model variability of the ratio of evaporation to runoff partitioning. Since the major runoff event takes place in the spring when snow is melting, the partition of the runoff into infiltration or runoff at this time contributes considerably to the annual water budget. They concluded that a detailed study during the melt period was needed to further address the reasons for these variations.

Slater et al. (2001) conducted a further detailed analysis of the snow schemes in these models and compared with observations from Valdai available then, and concluded that the

models are able to capture the broad features of the snow regime on intra- and interannual bases. They indicated that snow evaporation, snow albedo, and snow-cover fraction have a large impact on the snow simulations during ablation.

In spite of these previous analyses of the PILPS 2(d) experiment, the role of frozen soil schemes in affecting soil thermal properties, spring runoff, and infiltration has not been studied before. Different snow cover fraction formulations were discussed by Slater et al. (2001), but no observations were available then to evaluate these models. The objective of this study is to take advantage of PILPS 2(d) results that have not been analyzed before and new data sets to examine these issues. Specifically, we will focus on answering the following questions: 1) How well do land surface models with and without frozen soil schemes simulate soil temperature, and what is the impact of the frozen soil scheme on soil temperature simulations? 2) How well do land surface models simulate spring runoff and soil moisture, and what is the impact of the frozen soil scheme on the soil moisture and runoff simulations? 3) What is the role of the snow model in land surface modeling over cold regions?

In the next section we briefly summarize the observational data used in the experiment, and describe in detail new data that we have recently acquired and used for the first time. Section 3 gives the analysis, and discussion and conclusions are presented in Section 4.

2. Description of the Site and Data Sets

Descriptions of the continuous 18 years (1966-1983) of atmospheric forcing and hydrological data are given in detail by Vinnikov et al. (1996) and Schlosser et al. (1997). An overview of the dataset and a description of additional observational data are given below.

Table 2 lists the entire set of observations. We use most of them in this study. The data were obtained from the Valdai water-balance station (58.0°N, 33.2°E) located in a boreal forest region (Figure 1). Atmospheric data were measured at the meteorological site Priusadebny, in the central part of the Valdai Experimental Station, including temperature, pressure, and

humidity measured at 2 m, and wind speed at 10 m. The atmospheric data used as forcing by all the schemes were originally sampled at 3-hour intervals and were interpolated to 30-min intervals (or 5-min in some cases) using a cubic-spline interpolation procedure so that they could be utilized by the models. Downward shortwave radiation and downward longwave radiation were simulated based on observed cloudiness and temperature (Schlosser et al. 2000). The 21 LSSs were run for an 18-year period forced by these observations. The monthly averaged downward shortwave radiation varies from about 20 W m^{-2} in the winter to 290 W m^{-2} in the short summer each year (Figure 2). The strong seasonal cycle is mainly due to the large seasonal change of sun angle at this high latitude. The interannual variation of the downward shortwave radiation is strong during the 18 years, with the absolute variability greater in the summer than in winter. The amplitude of the interannual variation after removing the seasonal cycle can be up to 80 W m^{-2} on a monthly basis in the summer. The seasonal variation of the downward longwave radiation is much weaker than that of the downward shortwave radiation, but the interannual variation of longwave radiation has a larger amplitude during the winter rather than summer. This is because of the similar pattern for air temperature (Figure 2). The monthly average air temperature gets down to –10°C in January. The temperature threshold to separate snow from rainfall was specified as 0°C in this experiment (Schlosser et al. 2000), so most of the precipitation was snow during the winter. The precipitation shows some seasonality, varying from 1.5 mm/day to 3.5 mm/day on a monthly basis. The peak in October (Figure 2) is quite important, as it is the major source of soil moisture recharge before the snow covers the ground. Although precipitation has a small interannual variation during the winter, the interannual variation of snow depth is still rather large, as we will see in the next section. This can be attributed to the large interannual variation in air temperature and longwave radiation during the winter.

Long-term hydrological measurements were taken at the Usadievskiy catchment at Valdai, which has an area of about 0.36 km^2 and is covered with a grassland meadow (Figure 1). The Usadievskiy catchment is a few kilometers away from the meteorology station at Priusadebny. The hydrological data described by Vinnikov et al. (1996) and Schlosser et al. (1997, 2000) contain only the monthly-average evapotranspiration, runoff, liquid-water-equivalent snow depth (or, snow water equivalent, *SWE*), top 1-m soil moisture, and water table depth, which are only enough to study general features of the model performance on monthly and longer time scales. High-resolution observational data are needed to study processes with short time scales. We recently obtained additional daily observational data from Valdai, including daily soil temperature at different depths, soil moisture at different depths every 10 days, surface albedo when snow is present, and daily catchment discharge.

The discharge from the catchment was measured daily by a triangular weir and hydrometric flume at the catchment outflow site at Usadievskiy (Figure 1). If the water head at the weir did not exceed 100 mm, the discharge was calculated following an empirical relationship between heads and discharges for the catchment. The total discharge was converted to runoff rate by taking into account of the area of the catchment. We further modified the runoff to account for the monthly variations in the observed catchment-average water table depth following Schlosser et al. (1997). This is because the water table is very shallow at this catchment and the variation of the water table somewhat contributes to the discharge measured at the outflow site. However, this modification is relatively small. As we cannot separate the total runoff further into specific components, we compare this total runoff to the total runoff from the model simulations, which is the sum of the surface runoff, drainage from the root zone, and the lateral flow.

Soil moisture was measured using the gravimetric technique at 12 locations distributed over the Usadievskiy catchment (Figure 1), and the average of these 12 measurements is used.

The amount of water in each 10-cm soil layer down to 1 m was recorded at each measurement. The estimated error of this technique is about ±1 cm for the top 1-m soil moisture (Robock et al. 1995). Soil moisture was usually sampled three times a month, on the 8th, 18th, and 28th. Sometimes, especially when the ground is frozen, it was measured monthly on the 28th. Although only the root-zone (top 1-m in this catchment, as specified by Schlosser et al. (2000)) soil moisture was requested in the control run from the schemes, the multi-depth observations will help us understand the water flow inside the soil during the winter and the melting period. Since the observations are only taken three times a month, and in some cases only once a month, and soil moisture is a moisture reservoir and not a flux, the monthly averaged value is not really suitable for model evaluation. Therefore, as in many other studies, we use the soil moisture at the end of each month (i.e., on the 28th) to study the seasonal and interannual variations.

SWE was measured irregularly during the season at 44 locations inside the catchment (Figure 1) when snow was present and more frequently during snow ablation. The averaged number of measurement times each winter was about 13. The snow begins accumulating in late November each year and melts around the next April. The maximum snow depth and the time and duration of melting varied from year to year (Figure 3). Some other snow characteristics were also observed at Valdai during winter. The snow depth was measured whenever *SWE* was measured at the snow courses, and the snow density was derived from them. The snow cover fraction was also recorded based on all the snow measurements. Since this is a relative flat catchment covered with grass the snow cover fraction is 1 most of the winter, but it can vary dramatically during spring snow melt (Figure 4). The surface albedo was measured at the meteorological site Priusadebny approximately 4 km from the Usadievskiy catchment. It was measured with a pyranometer at about 1.5 m above the surface at local noon time. The pyranometer measured downward and upward shortwave radiation alternatively with the same sensor facing up and down. The field of view of the sensor is relatively small when it faces

downward due to its low mounting point. Therefore the representativeness of the surface albedo observation is unreliable for the catchment although the two sites are very close in distance and surface characteristics. For this reason, the surface albedo observations are not used in this study, but the data are introduced here.

The soil temperature was measured daily at the meteorology site at Priusadebny. Thermometers were placed vertically into the soil with the mercury bulbs at 20, 40, 80, and 120 cm below the surface and only extracted at the time of reading. The surface temperature was measured with a thermometer lying horizontally on the surface with the bottom half of the mercury bulb covered by soil or snow. If the surface was covered by snow, the thermometer was put on the snow surface. Therefore, it measured the snow surface temperature when snow was present and soil surface temperature at other times. We use these data, keeping in mind that they might differ slightly from the situation at the Usadievskiy catchment.

Besides the soil temperature, the depths of the top and bottom of the frozen soil layer were measured several times each winter at six locations inside the catchment (Figure 1). A plastic pipe filled with water was placed vertically into the soil. It was extracted from the soil at the time of observations to measure the position of the frozen layer. Even if soil temperature is relatively homogeneous over a small distance, the thickness of the frozen soil layers can have a much larger variation from one point to another due to naturally heterogeneous soil moisture fields. The spatial heterogeneity of soil moisture and frozen soil thickness, however, is beyond the scope of this study. We use the averaged thickness from five of those six observations to represent the catchment-averaged values while keeping in mind that this quantity has larger spatial variations (Figure 3). One observation was always very different from the other five, which makes it less representative of the whole catchment although the observation itself might be correct.

The maximum frozen soil thickness has a very large interannual variation (Figure 3). The soil froze to a depth of more than 500 mm in the winter of 1971-1972 but there was virtually no frozen soil in the winter of 1974-1975. There was a general tendency for the soil to be frozen more deeply when there was less snow and the temperature was colder, as expected. The correlation between the frozen depth and the snow depth is about 0.3, positive but relatively small.

3. Analysis

In this section, we first study soil temperature simulations. We compare models with a frozen soil scheme to those without and to observations, to understand the thermal effects of an explicit frozen soil scheme. Then the hydrological effects of the frozen soil scheme on infiltration are analyzed by comparing the soil moisture change and runoff simulations during spring snowmelt with the observations. The last part of this analysis focuses on the hysteresis of snow cover fraction and its impact on the snow simulation.

3.1 Soil temperature and thermal effects of frozen soil

Soil temperature is an important factor in land surface and atmospheric modeling. The soil surface temperature directly affects longwave radiation, sensible heat flux, and ground heat flux. A small error in soil temperature at the surface can introduce a large error in upward longwave radiation. The wrong soil temperature profile will produce the wrong ground heat flux, which in turn changes the energy budget at the surface and changes other energy terms, such as sensible and latent heat fluxes. Additionally, soil temperature denotes the existence of frozen soil. It also affects the initial snow accumulation at the soil surface. For all these reasons, correct soil temperature simulation is very important.

3.1.1 Soil temperature schemes and representation of thermal effect of frozen soil

Different approaches are currently implemented in different land surface models to simulate soil temperature and ground heat fluxes (Table 1). They can be simply grouped into the following 3 categories.

Zero-storage approach

This approach can be generally expressed by the following equation:

$$R_n - LE - H - G = 0 \tag{1}$$

where R_n [W/m^2] is net radiation, LE [W/m^2] is latent heat, H [W/m^2] is sensible heat and G [W/m^2] is ground heat flux. A typical bucket model uses this approach. It has only one soil layer in a hydrological sense and has no thermal layers, so the surface has no heat storage. The soil is assumed to be at a temperature that satisfies the energy balance at all times and there is no thermal capacity to the soil. Therefore there is no explicit soil temperature simulation. The ground heat flux is therefore ignored or prescribed in the energy budget. The usage of this approach is justified by the fact that the diurnal cycle of atmospheric forcing is removed.

Force-restore approach

This approach assumes periodic heating and uniform thermal properties of the soil; therefore it requires considerable modification and tuning over inhomogeneous soil (Dickinson 1988). Soil temperature changes are described by:

$$\begin{aligned} \frac{\partial T_s}{\partial t} &= \frac{1}{C_T}\left(R_n - H - LE\right) - \frac{2\pi}{\tau_1}\left(T_s - T_m\right) \\ \frac{\partial T_m}{\partial t} &= \frac{1}{\tau_1}\left(T_s - T_m\right) - \frac{2\pi}{\tau_2}\left(T_m - T_c\right) \end{aligned} \tag{2}$$

where t [s] is time, T_s [K] is the surface temperature, T_m [K] is the daily mean surface temperature, T_c [K] is the climatological deep temperature, C_T [J km^{-2}] is the surface soil/vegetation heat capacity per unit area, and τ_1 [s] and τ_2 [s] are time constants. In this particular form from ISBA (Mahfouf et al. 1995), T_s is restored toward the mean surface temperature T_m with a time constant τ_1 of 1 day, and T_m is restored toward the climatological

deep temperature T_c updated with a time constant τ_2 of 20 days. T_c is updated monthly. Using this approach, the model may have one or more layers. Since the soil temperature is restored toward climatology while allowing some degree of variation, if the climatological values are accurate, modeled soil temperature will not drift.

Heat conduction approach

This approach explicitly solves the heat conduction equation to get the soil temperatures for different model layers,

$$
\begin{aligned}
& C_s \frac{\partial T_g}{\partial t} = \frac{\partial}{\partial z}\left[\gamma \frac{\partial T_g}{\partial z}\right] \\
& G = \gamma \frac{\partial T_g}{\partial z}\Big|_{z=0} = R_n - LE - H \\
& G = \gamma \frac{\partial T_g}{\partial z}\Big|_{z=-h} = 0, \quad or \quad T_g\big|_{z=0} = T_s
\end{aligned}
\tag{3}
$$

where T_g [K] is the soil temperature at a particular layer, γ [J km^{-1}] is the soil thermal conductivity, and C_s [J km^{-2}] is the volumetric heat capacity of the soil. This approach might also have a layer with heat storage at the surface and not just an instantaneous energy balance. To solve the equation, the model needs to have several layers and to have them discretized in a proper way. Thermal capacities and thermal conductivity of all layers are needed to perform the calculation. This approach is considered to be the most realistic one. Many land surface models take this approach, such as PLACE (Wetzel and Boone 1995) and MAPS (Smirnova et al. 1997) (Table 2).

Because the requested output from models in this experiment is at the daily scale and the observations are also taken daily, we cannot evaluate the diurnal variation of soil temperature in this study.

3.1.2 Simulation of seasonal soil temperature variations

In PILPS 2(d), models provided average soil temperature for two overlapping layers, the upper layer (0-10 cm) and the lower layer (0-100 cm). The observations are at the surface and four individual depths. To avoid errors introduced by interpolation, we use the observed surface temperature and 20-cm soil temperature to compare with models' upper layer soil temperatures, and the observed 40-cm and 80-cm soil temperatures to compare with the models' lower layer. The surface temperature is really the snow surface temperature when snow is present during winter. For convenience, we also group the 21 models into two groups and plot them against observations separately in different panels.

The monthly averaged surface temperature can be lower than −10°C during winter (Figure 5) while the 20-cm soil temperature is very close to 0°C at the same time. The 40-cm and 80-cm soil temperatures are normally above 0°C on a monthly basis (Figure 6). Therefore, the largest temperature gradient exists between the surface temperature and the 20-cm level.

No matter which approach is used to simulate soil temperature in the models, the phase of the seasonal cycle of soil temperature is well captured for the upper layer, given the correct atmospheric forcing, especially air temperature (Figure 5a and 5b). The lower layer simulation, however, shows phase differences of up to about 1 month among models and between models and observations (Figure 6a and 6b).

The soil temperature shows a large scatter among models in both layers, especially during winter. Due to the framework of this comparison, we would expect the models' upper layer soil temperature to be bounded by the two observations at the surface and 20 cm, and the lower layer soil temperature to be bounded by the observations at 40 cm and 80 cm. The upper layer shows reasonably good agreement between models in group A and observations from April to November. Two models in group B overestimate the upper layer soil temperature during this period while others are reasonably good. During winter, models in group A have the upper layer soil temperature close to observations at 20 cm except the ISBA, MOSES, and NCEP models,

while models in group B have a much colder upper layer soil temperature, with exception of SSiB (Figure 5a and 5b). The lower layer soil temperature shows even larger differences between group A and group B (Figure 6a and 6b). The observed soil temperatures at 40 cm and 80 cm are very close to 0°C during winter. Almost all models in groups A (Figure 6a) produce very similar soil temperature simulations, but most of the models in group B (Figure 6b) produce much colder soil columns during winter and much warmer during summer time.

The aforementioned differences can be attributed to the existence of the frozen soil schemes. As indicated in Table 1 and in Figures 5-6 (group A are models with a frozen-water scheme and are plotted in solid lines in panels a and c, group B are models without a frozen-water scheme and are plotted in dashed lines in panels b and d), models with an explicit frozen soil scheme give a much more realistic soil temperature simulation during winter than those without a frozen soil scheme. Energy is released when the soil starts to freeze due to the phase change of water. The energy is then used to warm up the soil and to keep it from extreme cold. This simple mechanism works in the real world and in the models. So once a frozen soil scheme is included in a land surface model, the soil temperature will not get extremely cold at the lower and deep layers. This result would be best supported if we could rerun the simulations with the models that have a frozen soil scheme but with the scheme disabled. Since this study is a continuation of post-experiment analysis based upon the availability of new observational data set, and since models are continuously being improved, rerunning the same version of those models is not possible at this stage. However, these simple comparisons are already good evidence of the impact of a frozen soil scheme on soil temperature simulations.

3.1.3 Simulation of interannual variation of soil temperature

The observed surface temperature shows strong interannual variations while the other levels have a much weaker interannual variation during winter (Figures 5-6). As mentioned above, the observations show a general tendency for the soil to get very cold when snow is

thinner during winter. Nearly all models are able to capture this variability to some extent. Models with a frozen soil scheme have a much smaller amplitude of interannual variation for both layers (Figure 5c and 6c). They are also much closer to the amplitude of the observed variations. Models without a frozen soil scheme have a 3-5 times larger amplitude of variation compared to observations for the lower layer (Figure 5d and 6d).

3.1.4 Role of frozen soil schemes in soil temperature simulation

A physically-based frozen soil scheme releases energy as the soil water changes phase from liquid to solid. The energy slows the cooling of the soil to keep the surface temperature from becoming extremely cold at the beginning of the winter. The process of soil freezing effectively increases the thermal inertia of the soil at the beginning of winters, which efficiently damps large temperature variations from the surface down to the deep soil on all time scales.

Besides this direct effect, frozen soil schemes have another effect on soil temperature and ground heat flux simulations. The change of thermal conductivity of a soil column when soil water turns to ice is soil moisture-dependent. Generally speaking, as in the case of rather wet soil at Valdai during winter, frozen soil has a larger thermal conductivity than the unfrozen soil with the same water content due to the larger thermal conductivity of ice as compared to liquid water. The high thermal conductivity makes the heat transport inside the soil more efficient. Due to the downward temperature gradient (colder at the surface and warmer in the deep soil), the upward ground heat flux becomes larger when soil freezes. If this effect is also parameterized in the frozen soil scheme, it tends to cool the soil column, which makes the soil temperature lower (Smirnova et al. 2000). But this effect is probably weaker than the direct effect discussed above due to water phase changes.

Models with frozen soil all include the changes in heat capacity and thermal conductivity, but in slightly different ways. SWAP does this simply by changing the values by a certain factor when the soil is frozen. A more explicit method is to calculate the actually ice and water content

in the soil to determine the heat capacity and thermal conductivity (*e.g.*, CSIRO). Another important difference is how much liquid water models allow to exist when soil temperature is below 0°C. Some schemes do not allow liquid water to exist below 0°C, while others have liquid water inside the frozen soil layer (*e.g.*, MOSES, Cox et al. 1999). This difference eventually affects the soil temperature simulation, as well as hydraulic properties of the soil, as discussed later.

3.1.5 Model structure and soil temperature simulation

As shown in Figure 2 in Schlosser et al. (2000), the 21 participants have a wide range of the number of soil thermal layers, from the simplest 0 layers (BUCKET) to 14 layers (AMBETI, Braden 1995). A heat conduction approach needs at least 2 layers to solve the heat conduction equation. Ideally, the more layers and the thinner the layers get, the more chance there is to accurately simulate the soil temperature profile. However, practical accuracy is often limited by the absence of information on vertical profiles of parameters or even the vertical mean parameters. A thinner layer also requires a shorter time step. The balance between practical accuracy and efficiency is another factor that limits model performance. AMBETI has the best soil temperature simulation among all the models (not shown here). ISBA (Mahfouf et al. 1995, Noilhan et al. 1996) has only two thermal layers with the second one going from 10 cm to 2 m. The second layer soil temperature is fixed at 0°C when the top layer is frozen. This configuration produces large upward heat fluxes due to the large temperature gradient and thickness of the second layer. As discussed by Slater et al. (2001), the model structure, especially the way that the snow layer and top soil layer are connected, also affects the soil temperature simulation. An implicit scheme lumps snow and surface soil and vegetation together, so the soil temperature tends to be colder. This is different from models that diffuse energy between a separate snow layer and the top soil layer.

3.2 Runoff and soil moisture simulation in spring and the hydrological effect of a frozen soil scheme

As shown by Schlosser et al. (2000), nearly all models simulated the correct seasonal cycle of root-zone soil moisture fairly well, while at the same time there was considerable scatter among the models and there were differences between the models and the observations. Here, we will not study the soil moisture simulation during the whole period but rather focus on the winter and spring when frozen soil exists. Major runoff events happen during the spring snowmelt at Valdai, and we focus on this period for runoff, even though there is the second peak during the fall. Because of the large interannual variation of snow during winter and the snow ablation period in the spring, and the temporal scale of the runoff processes, mean values of snow and runoff calculated based on the 18 years are not good candidates to use in the study. Instead, we use several individual years as examples. Based on observations, the following three springs are chosen: 1972, 1976, and 1978. The winter of 1971-1972 had the least snow and the winter of 1975-1976 had the most snow during the 18 years. The winter of 1977-1978 had a snow depth close to the average over the 18 years. Looking at these three years gives us a more comprehensive picture of the models' performances.

3.2.1 Runoff simulation during snowmelt

As a consequence of the spring snowmelt, a large amount of water becomes available for infiltration and runoff. In the real world, if the infiltration capacity or the maximum infiltration rate is not large enough to let all the available water go into the soil, surface runoff will be generated. The infiltration capacity is controlled by the soil texture and soil moisture conditions. Whether the soil is frozen or not is another key factor that influences the infiltration capacity.

Largely influenced by the snow simulation, most models produce a slightly earlier runoff than observed (Figures 7-9). Generally, the earlier the snow ablation takes place in the model, the earlier the runoff will be; the faster the snow melts, the higher runoff peak will be observed;

and the more the snow amount, the more total volume of water available for runoff and infiltration. Sublimation also affects the partition of snow water. Slater et al. (2001) looked at the scatter in accumulated sublimation as simulated by models and found that net snow sublimation varies considerably among the models. This also affects the amount of snow available for runoff and infiltration when it melts. In this sense, the snow simulation has a large impact on the performance of the runoff simulation. In Figures 7-9 we highlight the model CROCUS in red in several panels. CROCUS gives a good simulation of snow in almost all years, especially of the timing of snowmelt. This in turn provides the correct amount of water to infiltration and runoff at the right time. The result is an almost perfect match to the runoff curves (Figures 7d-9d). This is especially important given the simplicity of the model's runoff scheme, where runoff rate is only determined by soil moisture with a linear relationship.

In addition to snow, the infiltration (or partition) scheme also affects the runoff. For example, model SPS (Kim and Ek 1995) has a satisfactory simulation of snow, but the runoff is totally wrong (Figures 7d-9d, green curves). This is simply because the model partitions all the meltwater into infiltration and drainage takes place much more slowly than surface runoff. The runoff peaks more than 20 days later than observed. The gradual release of water from the soil also reduces the maximum rate of runoff tremendously. The observed runoff rate can be as high as 15 mm/day, while SPS has a maximum runoff rate of 2-3 mm/day.

3.2.2 Soil moisture simulation

For the top 1 m of soil (Figures 7f-9f), all non-bucket type models can capture the soil moisture recharge after the snowmelt. Because at Valdai the top 1-m soil moisture is close to field capacity (specified as 271 mm in the PILPS 2(d) instructions) during most winters, the bucket is full and has no ability to accept any more water. For Richard's equation-based schemes, field capacity is not explicitly used and neither is the maximum of soil water content. One model (SPONSOR) seems to have a numerical instability problem during this simulation

(Figure 7g-9g, purple curves). A sudden soil moisture drop right after snowmelt might be caused by the extremely high hydraulic conductivity used in several time steps when soil becomes saturated with the melting water during the model integration. This soil moisture drop also produces a spike in total runoff simulation (Figure 7d-9d). This makes it not follow the seasonal cycle at all.

Observations show a soil moisture increase during snowmelt in most years, even though the top 1 m of soil is already close to or above field capacity. Then the soil moisture gradually decreases after the snow disappears. This means that there is infiltration taking place during snowmelt regardless of the soil moisture state before the melting or of the soil temperature. The water table temporarily enters the top 1 m of soil, making the soil moisture greater than the field capacity. This behavior for this part of Russia was previously pointed out by Robock et al. (1998) in their Figure 6.

For the top 10 cm soil (Figures 7e-9e), nearly all models underestimate the soil moisture. As shown in observations, the soil moisture in the top 10 cm is much higher than field capacity and very close to saturation. The total soil water content (including water and ice) decreases with depth almost linearly in the top 50 cm (not shown). This inverse soil moisture gradient was observed almost every September to the next April. This indicates that the surface soil layer might have a different porosity from the rest of the soil column, while the experiment uses the same porosity for all levels. The underestimation in the model simulation is due to the predefined soil porosity of 0.401 in the experiment, and therefore models cannot go above this.

3.2.3 Role of frozen soil scheme in the runoff and soil moisture simulation

In addition to the thermal effect of a frozen soil layer, discussed above, another potential effect is that when the soil is frozen or partially frozen, infiltration from the surface could be changed due to the change of soil structure, pore size distribution of the soil, and the hydraulic conductivity (Hillel 1998). The influence of freezing on soil structure varies depending on many

factors, such as structural condition before freezing, soil type, water content, number of freeze/thaw cycles, freezing temperature, and freezing rate. In soil with a poor structure, freezing can lead to a higher level of aggregation as a result of dehydration and the pressure of ice crystals. On the other hand, if the soil structure is well developed, expansion of the freezing water within the larger aggregates and clods may cause them to break down. This breakdown is enhanced when freezing occurs so fast that the water freezes in situ within the aggregates, whereas during slow freezing the water can migrate from the aggregates to the ice crystals in the macropores. Freezing influences the permeability of soils owing to the fact that ice impedes the infiltration rate. In partially frozen soil it is very likely that the infiltration rate will be suppressed as a result of impeding ice lenses as well as structural changes. Current land surface models do not simulate all these details but rather try to model a simplified process. An "explicit" frozen soil scheme will reduce the infiltration based on soil temperature, soil ice content, and soil properties. An "implicit" frozen soil scheme might totally stop water flow inside the soil (Mitchell and Warrilow, 1987) by specifying that if the snow melts while the soil is still frozen, the meltwater cannot infiltrate to recharge the soil moisture and it will have to run off. Models that are parameterized for general circulation model uses might not alter the infiltration capacity even when the soil is frozen. They are designed to represent a large region (one grid box in a low-resolution model) where Hortonian surface runoff from frozen soil surface would find its way into the soil elsewhere in the same grid box, owing to heterogeneities in frozen soil and soil freezing hydraulic conductivity (Cox et al. 1999). This will also help us to understand the difference in the runoff simulations shown between CROCUS and SPS. The latter is designed and calibrated to simulate processes at a much large spatial scale. This is why the runoff is delayed for about 20 days compared with observations. On the contrary, the simple runoff parameterization in CROCUS matches well the scale of this catchment so that it can

produce good simulations. We might speculate that the performance of these models would be different or even reversed when applied at the large scale for which SPS was developed.

Presumably, an LSS with a frozen soil scheme will have less water in the soil after the snow is gone, while those without frozen soil will fill the soil column with water and then let drainage and evaporation take place. But this speculation is based on two assumptions: 1) the soil is not saturated before the snowmelt so that infiltration can take place later on; 2) the soil is still totally frozen when snow is melting and there is no infiltration. In the PILPS 2(d) experiment, however, we do not see a big difference in soil moisture simulations from models with or without frozen soil physics. As mentioned above, the top 1 m of soil always reaches field capacity, and the top 10 or 20 cm can be saturated during winter in Valdai (Figures 7-9). The water table rises into the root zone at this time. No matter whether a frozen soil layer is included in a model or not, the change of soil moisture from before snow cover (normally November) to after the snowmelt is very limited by the available pore space. Nevertheless, the first assumption is valid in this case.

As shown in Figure 3, however, the soil ice is melting when the snow is melting. The top of the frozen soil layer moves downward to a lower level, which leaves the top part of the soil available for some infiltration. The winter of 1971-1972 is the winter with the least snow and thickest frozen soil. But when the snow melts, the frozen soil disappears from the top very quickly (Figure 3). As we mentioned above, the heterogeneity of soil freezing also allows surface water to find ways to infiltrate somewhere else in the catchment. The second assumption is invalid. Therefore, the influence of the frozen soil on infiltration is weak in the observations at Valdai. The difference in soil moisture simulations produced by frozen soil schemes between two groups of models (models with frozen soil and those without) cannot be clearly extinguished from the differences caused by any other sources of difference between models.

3.3 Snow cover fraction simulation and role of snow schemes in land surface modeling

The snow simulation in an LSS plays a very important role in the energy and water budget. The snow albedo changes the absorbed energy in the visible and near infrared bands dramatically at the surface. As discussed above, the total snow amount will determine the amount of available water for infiltration and runoff in spring. Slater et al. (2001) studied the snow simulations in this experiment and used the differences in snow evaporation, snow albedo, snow cover fraction, and snow model structure to explain the differences among the models. As an extension of their study, this paper will also address the snow cover fraction issue based on observations.

Surface albedo during winter depends on snow albedo, snow cover fraction and underlying vegetation. Snow albedo depends on the physical state of the snow, especially snow grain-size, snow type, and contamination. But these quantities are always hard to measure and quantify. Careful observations of snow albedo at small scales (*e.g.*, Warren and Wiscombe 1980, Warren 1982) have provided the basis for snow albedo simulation in numerical models. To explicitly simulate these processes by solving a full set of equations is computationally expensive, so most land surface models take a shortcut, using empirical relationships between snow albedo and other variables, such as temperature, age of snow, and *SWE*. Different snow models may only consider a subset of these in the snow albedo formulation. The snow cover fraction is formulated as a linear or asymptotic function based on snow depth and surface characteristics such as vegetation roughness. Of course, the simplest model is to assume 100% coverage of snow when snow is present. Detailed information about albedo and fractional cover formulas in the 21 LSSs in PILPS 2(d) is listed in Table 2 of Slater et al. (2001).

SWE and snow cover fractions were observed at 44 points inside the catchment so they more or less represent the whole catchment. The observed snow cover fraction was 100% from the first observation during winter to the beginning of snowmelt (Figures 7d-9d). Even with thin snow on the ground after the initial snowfall, the snow cover fraction was high and the surface

albedo was high. When models cannot correctly simulate snow cover fraction, the surface albedo will be wrong even with a correct snow albedo scheme. During snowmelt, with a fair amount of snow on the ground, the surface albedo can be very low because the snow cover fraction is low and because of a low snow albedo when melting.

Because fresh snow has a much higher albedo than old snow, snow albedo exhibits hysteresis in the relationship between total snow depth and snow albedo even though it is the surface layer of snow that determines snow albedo. This hysteresis can be represented in models that explicitly simulate the snow albedo based on the top snow layer. Interestingly, the snow cover fraction at the Valdai grassland also exhibits hysteresis. For the same amount of snow, snow cover fraction during snow accumulation is always higher than during the snowmelt period, especially for thin snow. As shown in Figure 4b, there is a general linear relationship between *SWE* and snow-cover fraction when snow covers less than 100% of the area. This linear relationship is from observations during snowmelt and we can speculate that the relationship between those two during snow accumulation will have a smaller slope.

To illustrate this snow cover fraction hysteresis, the numbered arrows in Figure 4b indicate the possible path of changes of snow cover fraction and *SWE* during a winter. Arrow 1 is the first snowfall at the beginning of the winter or late fall. This is a dramatic change in surface albedo and snow cover fraction without heavy snowfall. Arrow 2 is during the snow accumulation period, which lasts about 4 months. Arrow 3 is during the first several days of the melting when *SWE* decreases quickly while the snow still covers the whole area. After that, snow-cover fraction decreases almost linearly with *SWE* as indicated by arrow 4. If there is another snowfall during the melting period, it brings the snow cover fraction back to 1.0 very quickly even though this snowfall might be little. This effect is very well illustrated in 1976 (Figures 8b-c). As a result of the late season snowfall and subsequent increase of snow cover fraction, we expect the surface albedo to jump right up after the snowfall. Then the snow cover

fraction decreases linearly with *SWE* again until all the snow is gone. It is easy to fit the data to get an empirical function at this stage, but this linear relation is probably not universal and depends somewhat on the surface topography and vegetation. Since none of the snow cover fraction formulas in the current models include this feature, the lack of this effect can significantly affect the snow simulations.

4. Discussion and Conclusions

The 18-year off-line simulations and observations from Valdai with inter- and intra-annual variation of soil temperature, frozen soil depth, soil moisture, snow, and runoff are a valuable resource for land surface model validation and evaluation. It must be remembered, however, that the model simulations used in this analysis were conducted several years ago. Some of the models have been improved since then, including improvements in response to the results of this PILPS 2(d) experiment, and therefore the results may not reflect the current model performance. Most of these models also participated in the PILPS 2(e) experiment and their current performance in cold region simulations is described by Bowling et al. (2002a), Nijssen et al. (2002) and Bowling et al. (2002b). In PILPS 2(e) most models include an explicit representation of frozen soil, no doubt partly in response to the results of PILPS 2(d). We hope, however, that the new analyses presented here will lead to further improvement of model performances.

Over a region like Valdai with seasonal snow cover and frozen soil, snow simulation is the most important feature for a land surface model to be able to simulate components of the land surface hydrology correctly in the spring. Snow affects the availability of water for runoff and infiltration, affects the energy available for evapotranspiration through its albedo and indirect effect on resulting soil moisture, and affects soil temperature by its blanketing effects. These effects are clearly demonstrated in the analyses of the PILPS 2(d) experiment here.

Based on observations, snow metamorphism has been introduced into some snow modules. Physical processes such as absorption of solar radiation with depth, phase changes between solid and liquid water, and water transmission through the snowpack have been added (*e.g.*, CROCUS, Brun et al. 1992). Brun et al. showed that introduction of metamorphism laws into the snow model significantly improved model performance. We also showed that more sophisticated snow schemes in land surface models after careful calibration have the potential to produce a large improvement in hydrological event simulations in a region where snow cover lasts several months and water equivalent snow depth reaches several cm. Simple snow models can simulate snow accumulation when the right critical temperature for snowfall is chosen, but once snow starts to melt, they do not have the ability to represent the real world, resulting in errors in the simulation of snow melting in terms of timing and total amount. Although there are tunable parameters in simple snow models in most cases, and there is always the possibility that the model can be tuned to fit observations, the parameter values would have to be case- and region-dependent, and even then the model would not capture the real physics. A realistic parameterization of snow cover fraction that relates the surface characteristics and represents the hysteresis is needed to improve the snow and surface energy simulation. We have observed this important feature in the grassland catchment, but none of the models parameterizes it into the snow model. This can potentially produce substantial errors in surface albedo simulation and energy budget.

Frozen soil in the winter was expected to have a great influence on the runoff and soil moisture simulation (Mitchell and Warrilow 1987, Pitman et al. 1999). But Pitman et al. (1999) were not able to show improvement of runoff simulation when including soil ice in a Global Soil Wetness Project-type simulation. Cherkauer and Lettenmaier (1999) also found that including frozen soil in their LSS had a relatively small effect on soil moisture and runoff. Even though snow is present, infiltration can occur as the soil is not frozen near the top as meltwater

percolates. Over a large region, Hortonian surface runoff can always find its way to infiltrate somewhere in the domain owning to the fact that soil is not freezing homogeneously because of variation in soil texture, soil structure, soil moisture and soil temperature, and many other factors. So inclusion of a frozen soil scheme has little effect on the simulations of soil moisture.

Soil water freezing has been proved to be very important in soil temperature simulation, however. We observed a large temperature gradient at the near surface soil during winter. This is attributed to the frozen soil, which releases heat when water changes phases from liquid to solid, keeping the soil from getting extreme cold. This effect is also found in models with a frozen soil scheme, in both seasonal and interannual time scales. These models produce much more realistic soil temperature variations than those without a frozen soil scheme. It has been found that soil temperature is a dominant factor in determining the rate of soil carbon cycling in the boreal forest (Nakane et al. 1997), and the timing of snowmelt and soil thaw is a major factor in determining annual carbon uptake in a boreal region (Sellers et al., 1997). As land surface schemes begin to simulate carbon and nitrogen fluxes from biological processes, they need to get soil freezing and soil temperature right to be able to correctly simulate the biological processes. Our results suggest that with a more explicit frozen soil model they have the hope of doing so.

Acknowledgments. We thank Nina Speranskaya for the new Valdai data. We thank three anonymous reviewers for valuable recommendations. Figures were drawn with GrADS, created by Brian Doty. This work is supported by NOAA grants NA56GPO212, NA96GPO392, and GC99-443b, and the New Jersey Agricultural Experiment Station.

References

Bowling et al., 2002a: Simulation of high latitude hydrological processes in the Torne-Kalix basin: PILPS Phase 2(e), 1: Experiment description and summary intercomparisons. *Glob. Plan. Change*, in press.

Bowling et al. 2002b: Simulation of high latitude hydrological processes in the Torne-Kalix basin: PILPS Phase 2(e), 3: Equivalent model representation and sensitivity experiments. *Glob. Plan. Change*, in press.

Braden, H., 1995: The model AMBETI, A detailed description of a soil-plant-atmosphere model. *Berichte des Deutschen Wetterdienstes*, **195**, 113 pp.

Brun, E., P. David, and M. Sudul, 1992: A numerical model to simulate snow-cover stratigraphy for operational avalanche forecasting. *J. Glaciol*., **38**, 13-22.

Budyko, M. I., 1956: *Heat Balance of the Earth's Surface*, Gidrometeoizdat, Leningrad, 255 pp. (in Russian)

Cherkauer, K. A., and D. P. Lettenmaier, 1999: Hydrologic effects of frozen soils in the upper Mississippi River basin, *J. Geophys. Res.*, **104**, 19,599-19,610.

Cox, P. M., R. A. Batts, C. B. Bunton, R. L. H. Essery, P. R. Rowntree, and J. Smith, 1999: The impact of new land surface physics on the GCM simulation of climate and climate sensitivity. *Clim. Dyn*., **15**, 183-203.

Dai, Y.-J., and Q.-C. Zeng, 1997: A land-surface model (IAP94) for climate studies. Part I: Formulation and validation in off-line experiments. *Adv. Atmos. Sci*., **14**, 433-460.

de Rosnay, P., J. Polcher, M. Bruen, and K. Laval, 2002: Impact of a physically based soil water flow and soil-plant interaction representation for modeling large scale land surface processes. *J. Geophy. Res.*, in press.

Desborough, C. E., and A. J. Pitman, 1998: The BASE land surface model. *Global Planet. Change*, **19**, 3-18.

Dickinson, R. E., 1988: The force-restore model for surface temperatures and its generalizations. *J. Climate*, **1**, 1086-1097.

Gedney, N., P. M. Cox, H. Douville, J. Polcher, and P. J. Valdes, 2000: Characterizing GCM land surface schemes to understand their responses to climate change. *J. Clim.*,**13**,3-66-3079.

Henderson-Sellers, A., Z.-L. Yang, and R. E. Dickinson, 1993: The Project for Intercomparison of Land-surface Parameterization Schemes. *Bull. Amer. Meteor. Soc.*, **74**, 1335-1350.

Henderson-Sellers, A., A. J. Pitman, P. K. Love, P. Irannejad, and T. H. Chen, 1995: The Project for Intercomparison of Land-surface Parameterization Schemes (PILPS): Phases 2 and 3. *Bull. Amer. Meteor. Soc.*, **76**, 489-504.

Hillel, D., 1998: *Environmental Soil Physics*. Academic Press, New York, 771 pp.

Kim, J., and M. Ek, 1995: A simulation of the surface energy budget and soil water content over the HAPEX-MOBILHY forest site. *J. Geophys. Res.*, **100**, 20,845-20,854.

Mahfouf, J-F., A. O. Manzi, J. Noilhan, H. Giordani, and M. Déqué, 1995: The land surface scheme ISBA within the Météo-France Climate Model ARPEGE. Part I: implementation and preliminary results. *J. Climate*, **8**, 2039-2057

Manabe, S., 1969: Climate and the ocean circulation, 1. The atmospheric circulation and the hydrology of the earth's surface. *Mon. Wea. Rev.*, **97**, 739-774.

Mitchell, J. F. B., and D. A. Warrilow, 1987: Summer dryness in northern mid-latitudes due to increased CO_2. *Nature*, **341**, 132-134.

Nakane, K., T. Kohno, T. Horikoshi and T. Nakatsubo, 1997: Soil carbon cycling at a black spruce (Picea mariana) forest stand in Saskatchewan, Canada. *J. Geophys. Res.*, **102,** 28,785-28,793.

Nijssen et al., 2002: Simulation of high latitude hydrological processes in the Torne-Kalix basin: PILPS Phase 2(e), 2: Comparison of model results with observations. *Glob. Plan. Change*, in press.

Noilhan, J., and J.-F. Mahfouf, 1996: The ISBA land surface parameterization scheme. *Global Planet. Change*, **13**, 145-159.

Pitman, A. J., A. G. Slater, C. E. Desborough, and M. Zhao, 1999: Uncertainty in the simulation of runoff due to the parameterization of frozen soil moisture using the Global Soil Wetness Project methodology. *J. Geophys. Res*., **104**, 16,879-16,888.

Robock, A., K. Y. Vinnikov, C. A. Schlosser, N. A. Speranskaya, and Y. Xue, 1995: Use of midlatitude soil moisture and meteorological observations to validate soil moisture simulations with biosphere and bucket models. *J. Climate*, **8**, 15-35.

Robock, A., C. A. Schlosser, K. Y. Vinnikov, N. A. Speranskaya, and J. K. Entin, 1998: Evaluation of AMIP soil moisture simulations. *Glob. Plan. Change*, **19**, 181-208.

Sellers, P. J., F. G. Hall, R. D. Kelly, A. Black, D. Baldocchi, J. Berry, M. Ryan, K, J. Ranson, P. M. Crill, D. P. Lettenmaier, H. Margolis, J. Cihlar, J. Newcomer, D. Fitzjarrald, P. G. Jarvis, S. T. Gower, D. Halliwell, D. Williams, B. Goodison, D. E. Wickland and F. E. Guertin: BOREAS in 1997: Experiment overview, scientific results and future directions. *J. Geophys. Res.*, **102**, 28,731-28,769.

Schlosser, C. A., A. Robock, K. Y. Vinnikov, N. A. Speranskaya, and Y. Xue, 1997: 18-Year land-surface hydrology model simulations for a midlatitude grassland catchment in Valdai, Russia. *Mon. Weather Rev*., **125**, 3279-3296.

Schlosser, C. A., A. G. Slater, A. Robock, A. J. Pitman, K. Y. Vinnikov, A. Henderson-Sellers, N. A. Speranskaya, K. Mitchell, and the PILPS 2(d) contributors, 2000: Simulations of a boreal grassland hydrology at Valdai, Russia: PILPS Phase 2(d). *Mon. Weather Rev*., **128**, 301-321.

Shmakin, A. B., 1998: The updated version of SPONSOR land surface scheme: PILPS-influenced improvements. *Glob. Plan. Change,* **19**, 49-62.

Slater A. G., A. J. Pitman, and C. E. Desborough, 1998: The validation of a snow parameterization designed for use in general circulation models. *Internat. J. Climatology*, **18**, 595-617.

Slater, A. G., C. A. Schlosser, C. E. Desborough, A. J. Pitman, A. Henderson-Sellers, A. Robock, K. Ya. Vinnikov, N. A. Speranskaya, K. Mitchell, A. Boone, H. Braden, F. Chen, P. M. Cox, P. de Rosnay, R. E. Dickinson, Y-J. Dai, Q. Duan, J. Entin, P. Etchevers, N. Gedney, Ye. M. Gusev, F. Habets, J. Kim, V. Koren, E. A. Kowalczyk, O. N. Nasonova, J. Noilhan, J. Schaake, A. B. Shmakin, T. G. Smirnova, D. Verseghy, P. Wetzel, Y. Xue, Z-L. Yang, and Q. Zeng, 2001: The representation of snow in land-surface schemes: Results from PILPS 2(d). *J. Hydrometeorology*, **2**, 7-25.

Smirnova, T. G., J. M. Brown, and S. G. Benjamin, 1997: Performance of different soil model configurations in simulating ground surface temperature and surface fluxes. *Mon. Weather Rev*., **125**, 1870-1884.

Smirnova T. G., J. M. Brown, S. G. Benjamin, and D. Kim, 2000: Parameterization of cold-season processes in the MAPS land-surface scheme. *J. Geophys. Res.*, **105**, 4077-4086.

Verseghy, D., N. McFarlane, and M. Lazare, 1991: CLASS – A Canadian Land Surface Scheme for GCMs. Part I: Soil model. *Int. J. Climatol*., **11**, 111-133.

Vinnikov, K. Y., A. Robock, N. A. Speranskaya, and C. A. Schlosser, 1996: Scales of temporal and spatial variability of midlatitude soil moisture. *J. Geophys. Res.*, **101**, 7163-7174.

Warren, S. G., 1982: Optical properties of snow. *Rev. Geophys. Space Phys.*, **20**, 67-89.

Warren, S. G, and W. J. Wiscombe, 1980: A model for the spectral albedo of snow. II: Snow containing atmospheric aerosols. *J. Atmos. Sci.*, **37**, 2734-2745.

Wetzel, P., and A. Boone, 1995: A parameterization for land–atmo-sphere–cloud exchange (PLACE): Documentation and testing of a detailed process model of the partly cloudy boundary layer over heterogeneous land. *J. Climate*, **8**, 1810-1837.

Xue, Y., P. J. Sellers, J. L. Kinter, and J. Shukla, 1991: A simplified biosphere model for global climate studies. *J. Climate*, **4**, 345-364.

Yang, Z.-L., R. E. Dickinson, A. Robock, and K. Ya. Vinnikov, 1997: Validation of the snow submodel of the Biosphere-Atmosphere Transfer Scheme with Russian snow cover and meteorological observational data. *J. Climate*, **10**, 353-373.

Table 1. Participating land surface schemes. Schlosser et al. (2000) gives references for all the PILPS 2(d) schemes. Soil temperature: ZS: zero-storage, FR: force-restore, HC: heat conduction.

	Model	Contact(s)	Soil temperature	Frozen soil?
1	**AMBETI**	H. Braden	HC	Yes
2	**BASE**	A. Slater C. Desborough A. Pitman	HC	Yes
3	**BATS**	Z. L. Yang R. E. Dickinson	FR	No
4	**BUCKET**	C.A. Schlosser	ZS	No
5	**CLASS**	D. Verseghy	HC	Yes
6	**CROCUS**	P. Etchevers	HC	No
7	**CSIRO**	E. Kowalczyk	HC	Yes
8	**IAP94**	Y. Dai	HC	Yes
9	**ISBA**	F. Habets J. Noilhan	FR	Yes
10	**MAPS**	T. Smirnova	HC	No
11	**MOSES**	P. Cox	HC	Yes
12	**NCEP**	K. Mitchell Q. Duan	HC	Yes
13	**PLACE**	A. Boone, P. Wetzel	HC	No
14	**SECHIBA2**	P. de Rosnay J. Polcher	HC	No
15	**SLAM**	C. Desborough	HC	Yes
16	**SPS**	J. Kim	HC	Yes
17	**SPONSOR**	A. B. Shmakin	HC	Yes
18	**SSiB**	Y. Xue C.A. Schlosser	FR	No
19	**SWAP**	Y. M. Gusev O. N. Nasonova	FR/ZS	Yes
20	**UGAMP**	N. Gedney	HC	No
21	**UKMO**	P.Cox	HC	No

Table 2. Observational data set at Valdai.

Meteorological data from meteorological station Priusadebny, taken every 3h, 1966-1983
Precipitation
2-m air temperature
Pressure
Humidity
Wind speed
Hydrological data from Usadievskiy catchment
Total soil moisture in the top every 10 cm down to 1 m depth: once to three times per month, 1966-1985
Discharge, daily, 1966-1985
Depth of groundwater table, monthly, 1960-1990
Water equivalent snow depth, irregularly, 1960-1990
Soil surface evaporation, 10-day period sum from late spring to early autumn, 1966-1985
Snow cover fraction, snow thickness and snow density irregularly, 1966-1985
Freezing/melting depth, irregularly, 1966-1985
Groundwater depth, every 5 days at different sites inside the catchment, 1966-1985
Data from Meteorological station (Priusadebny)
Soil surface temperature, daily, 1967, 1971-1985
Soil temperature at 20 cm, 40 cm, and 80 cm, daily, 1967, 1971-1985
Soil surface evaporation, 10-day period sum from late spring to early autumn, 1966-1985
Surface albedo, irregularly, 1966-1985

List of Figures

Figure 6. Same as Figure 5, but for the top 0-100 cm soil temperature from models. The observations are at depths of 40 and 80 cm.

Figure 7. Time series of the major hydrological variables simulated by models for the winter of 1971-1972. a) Precipitation (mm/day). Blue indicates snowfall and red indicates rain. b) Snow water equivalent (*SWE*, mm). Blue dots indicate observations. Models are plotted as black lines except CROCUS and SPS, which are highlighted in red and green, respectively. c) Snow-cover fraction (%). Only observations are available. d) Daily runoff (mm/day). Blue curve is the observations. Models are plotted as black curves except CROCUS, SPS and SPONSOR, which are highlighted in red, green and purple, respectively. e) Top 10-cm soil moisture (SM) (mm). Blue dots are observations. Models are plotted as black curves except CROCUS, which is highlighted in red. SPS and SPONSOR do not have output for this layer. Model simulations of 0-10 cm soil moisture are only available from February to May in 1971 to 1979. f) As in e, but for top 1-m. Models are plotted as black curves except CROCUS, SPS and SPONSOR, which are highlighted in red, green and purple, respectively.

Figure 8. Same as Figure 7, but for the winter of 1975-1976.

Figure 9. Same as Figure 7, but for the winter of 1977-1978.

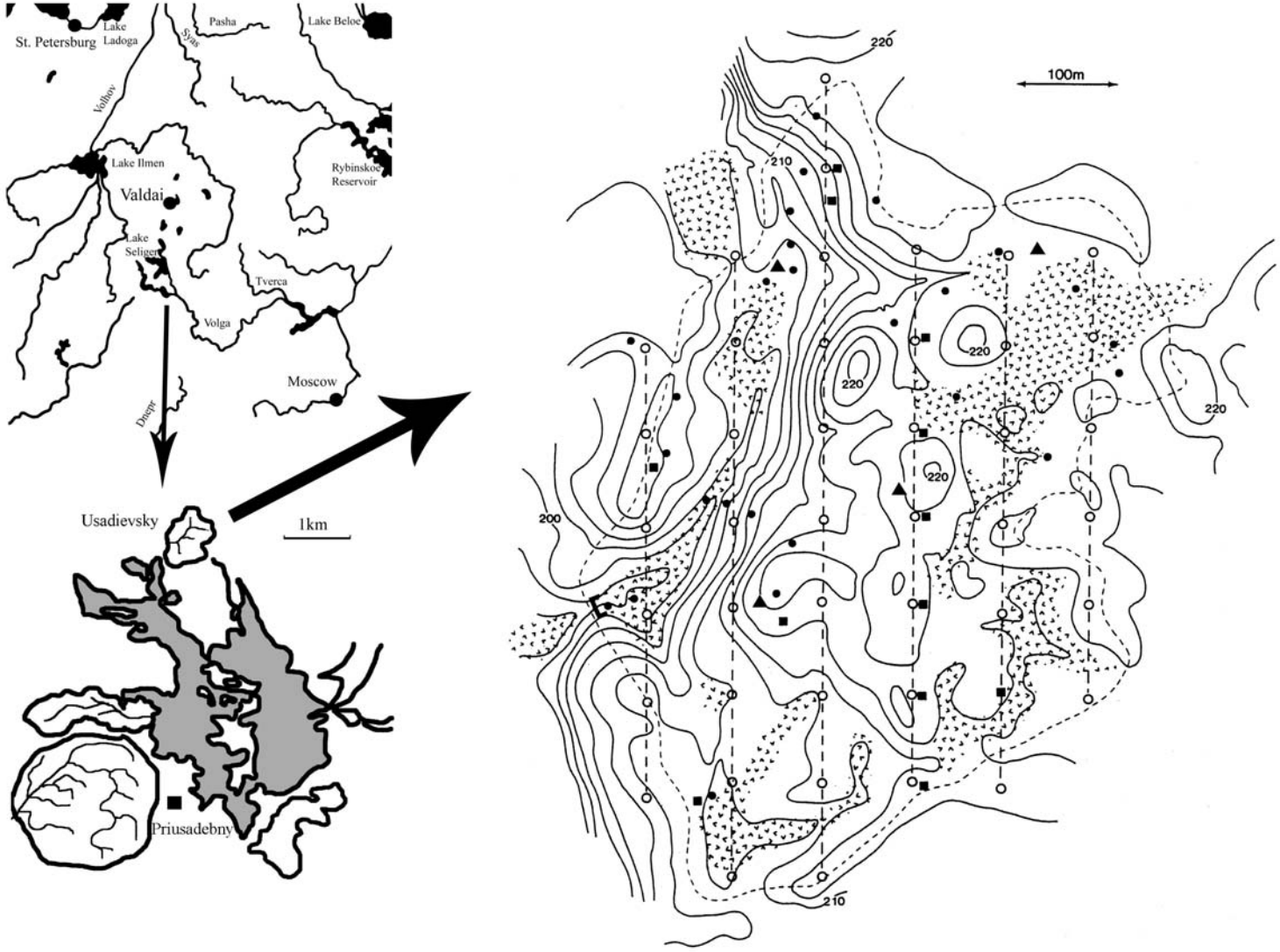

Figure 1. Map of the Usadievskiy catchment at Valdai and geographical location of the catchment, modified from Figure 1 in Schlosser et al. (1997). Water-table measurement sites are indicated by filled circles. Open circles with dashed lines indicated the snow measurement sites and routes, respectively. Discharge is measured at the stream outflow point of the catchment located in the lower left-hand corner of the catchment map and indicated by a bold bracket. Filled triangles indicate the measurement sites of soil freezing and thawing depths.

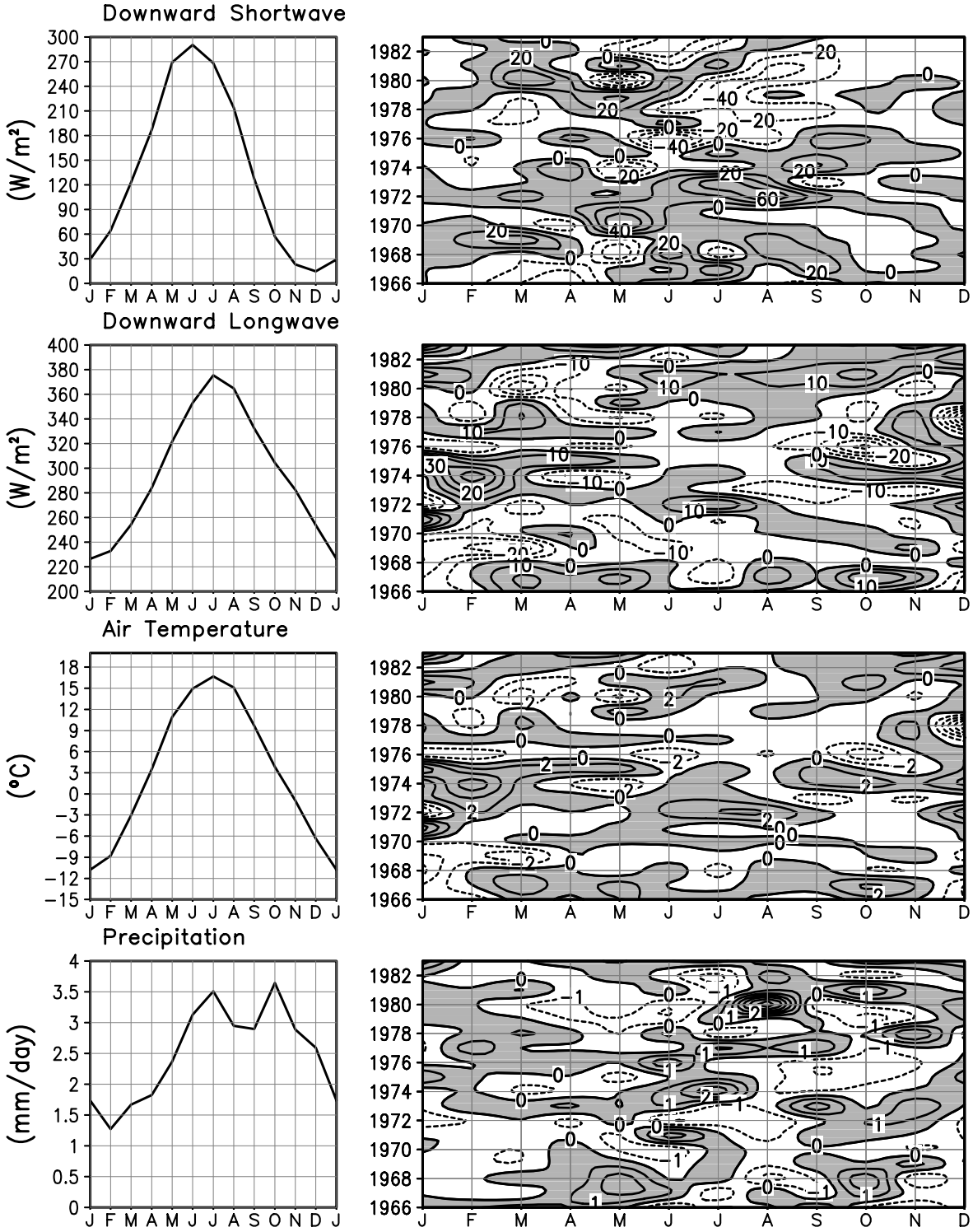

Figure 2. Seasonal and interannual variation of the major atmospheric forcings on a monthly scale in the PILPS 2(d) experiment. The mean seasonal cycles are in the panels on the left and the monthly and seasonal anomalies are contoured on the right.

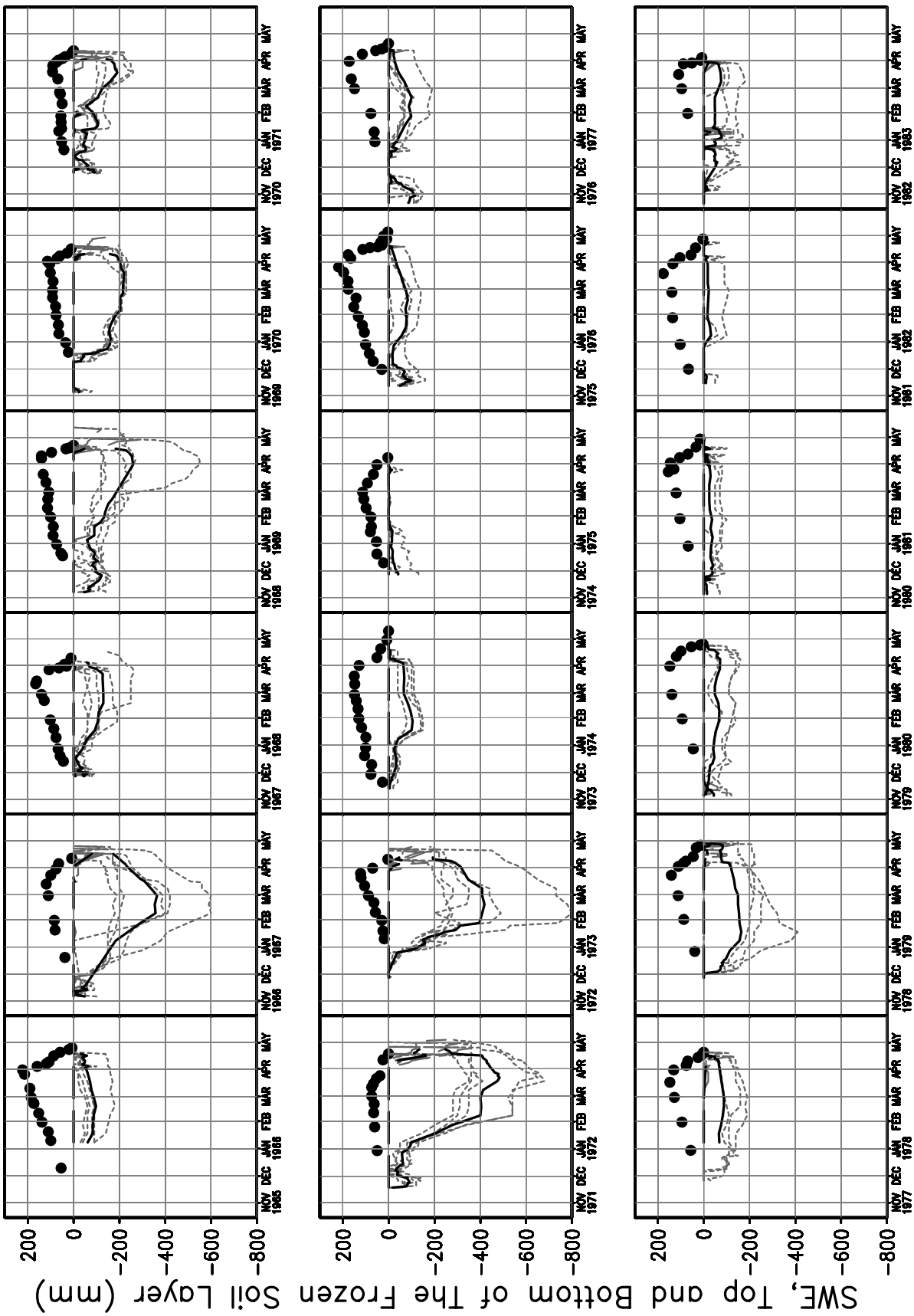

Figure 3. Observed time series of snow water equivalent (*SWE*, mm, circles) and the depths (mm) of the top and bottom of the frozen soil layer for each year. The gray dashed lines are observations from each individual location and the black lines are the average.

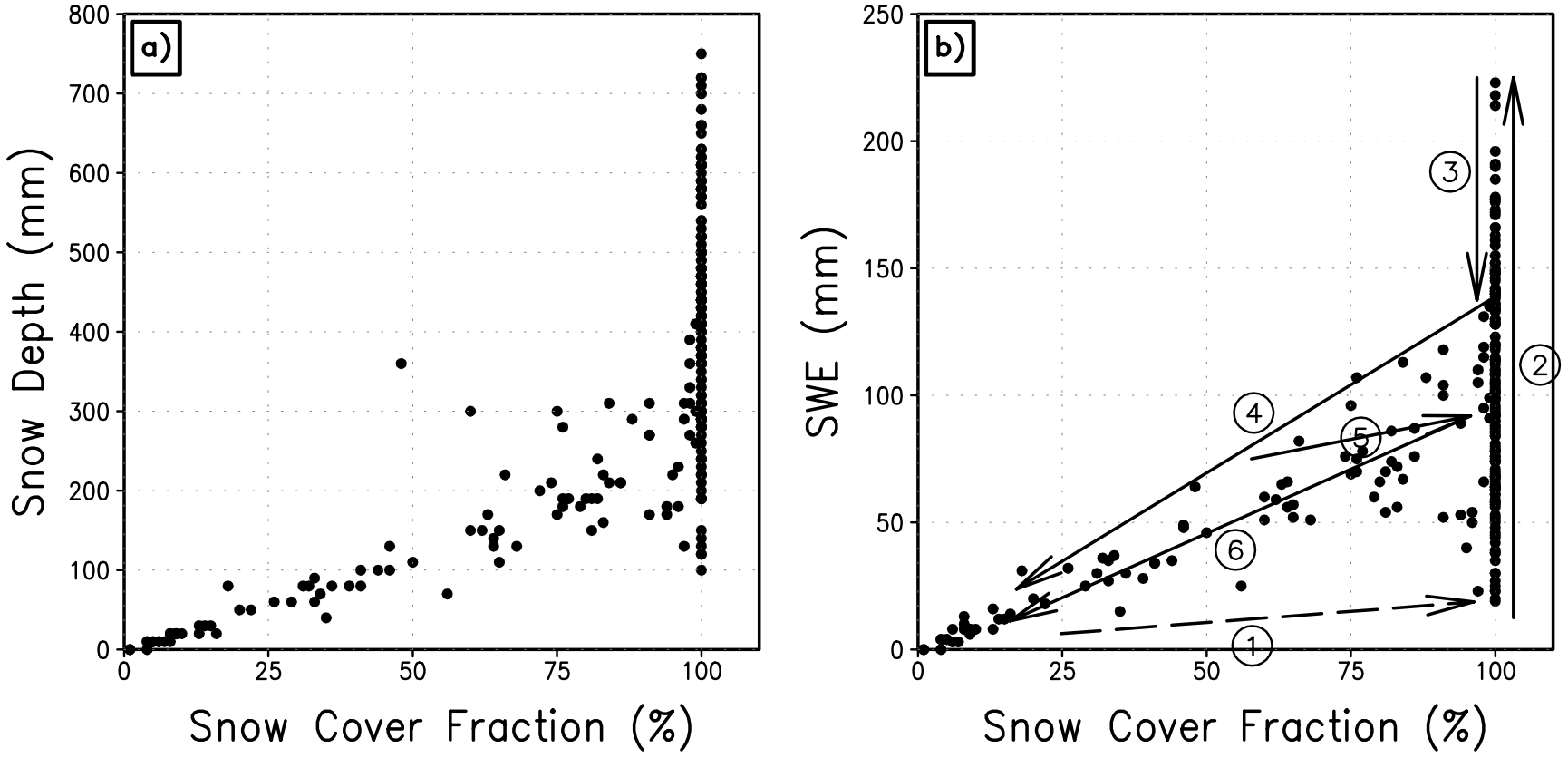

Figure 4. The observed relationship between a) snow water equivalent (*SWE*) and snow albedo, b) snow-cover fraction and snow depth, c) surface albedo and snow cover fraction, and d) *SWE* and snow cover fraction. The numbered arrows indicate the possible path of changes of snow cover fraction and *SWE* during a winter. See text for discussion. Observations are shown for the entire 18-year period at Valdai. The albedo observations are from one point only at Valdai, and may not be representative of the entire catchment average.

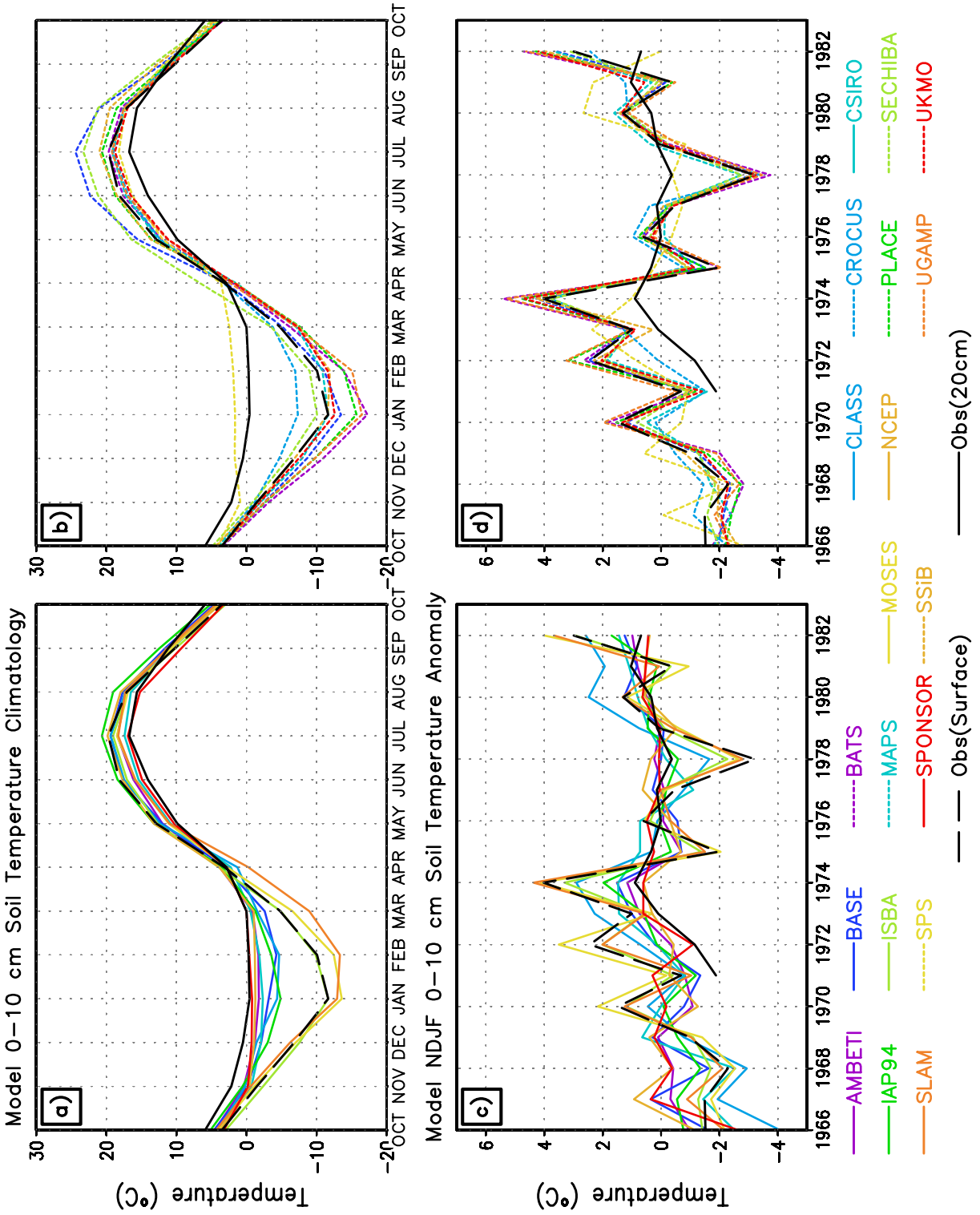

Figure 5. The mean seasonal cycle of the 0-10 cm soil temperature from all models compared with observations at the surface and 20 cm (top panels). Interannual anomalies of the 0-10 cm soil temperature averaged for the November-February period from all models compared with observations (bottom panels). Models with frozen soil schemes are plotted in solid lines in panels a and c while models without are plotted with dashed lines in panels b and d.

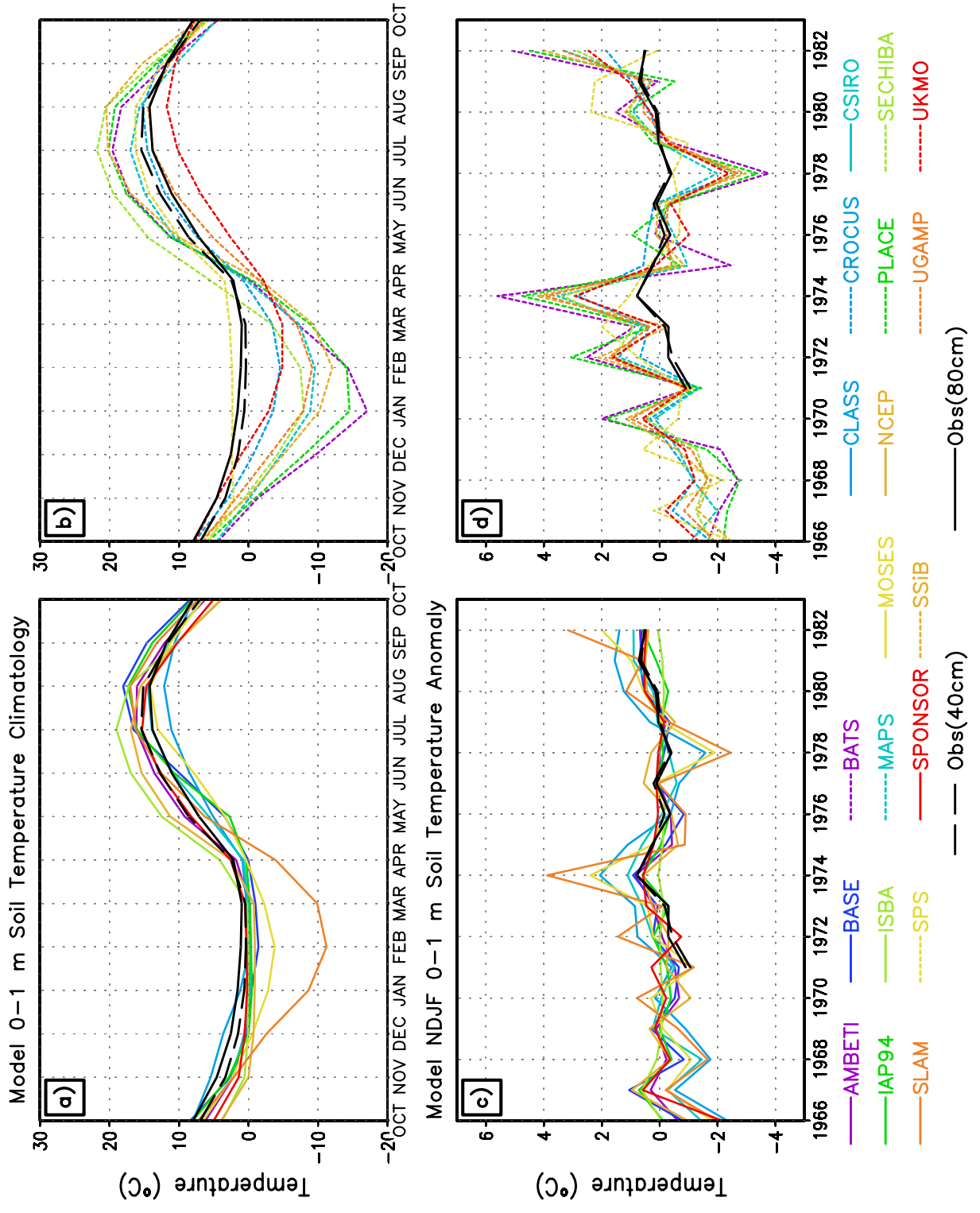

Figure 6. Same as Figure 5, but for the top 0-100 cm soil temperature from models. The observations are at depths of 40 and 80 cm.

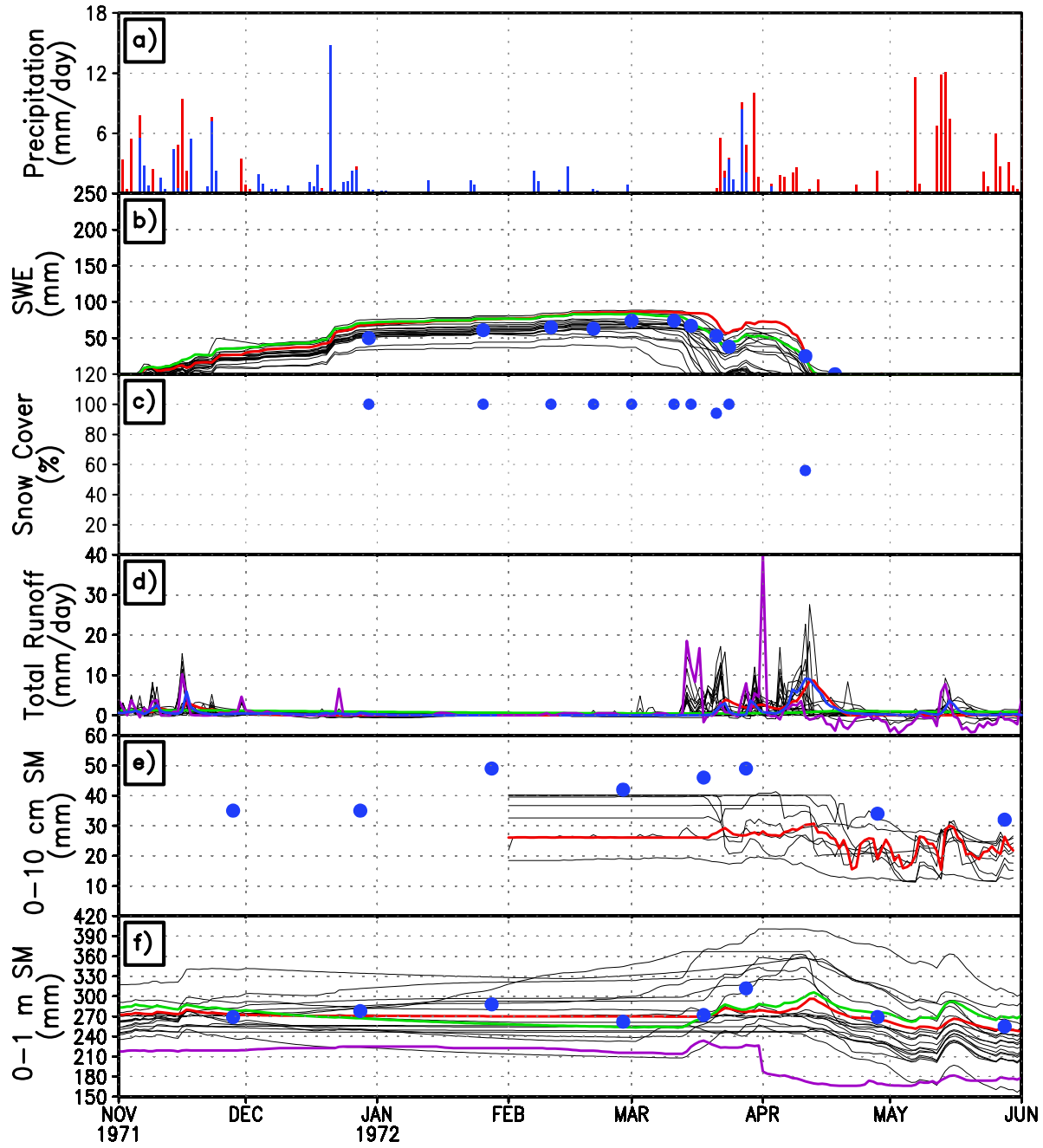

Figure 7. Time series of the major hydrological variables simulated by models for the winter of 1971-1972. a) Precipitation (mm/day). Blue indicates snowfall and red indicates rain. b) Snow water equivalent (SWE, mm). Blue dots indicate observations. Models are plotted as black lines except CROCUS and SPS, which are highlighted in red and green, respectively. c) Snow-cover fraction (%). Only observations are available. d) Daily runoff (mm/day). Blue curve is the observations. Models are plotted as black curves except CROCUS, SPS and SPONSOR, which are highlighted in red, green and purple, respectively. e) Top 10-cm soil moisture (SM) (mm). Blue dots are observations. Models are plotted as black curves except CROCUS, which is highlighted in red. SPS and SPONSOR do not have output for this layer. f) As in e, but for top 1-m. Models are plotted as black curves except CROCUS, SPS and SPONSOR, which are highlighted in red, green and purple, respectively.

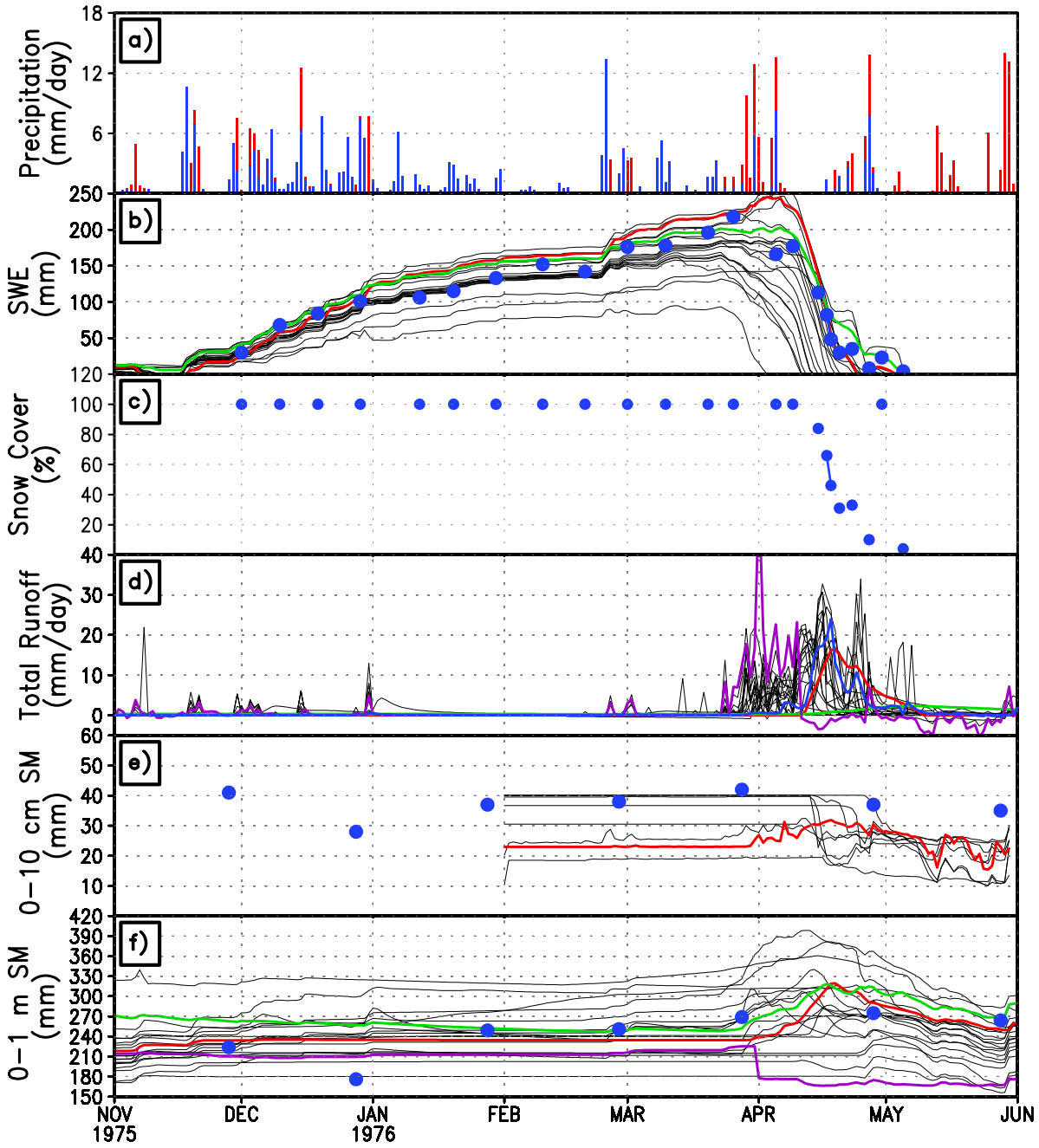

Figure 8 Same as Figure 7, but for the winter of 1975-1976.

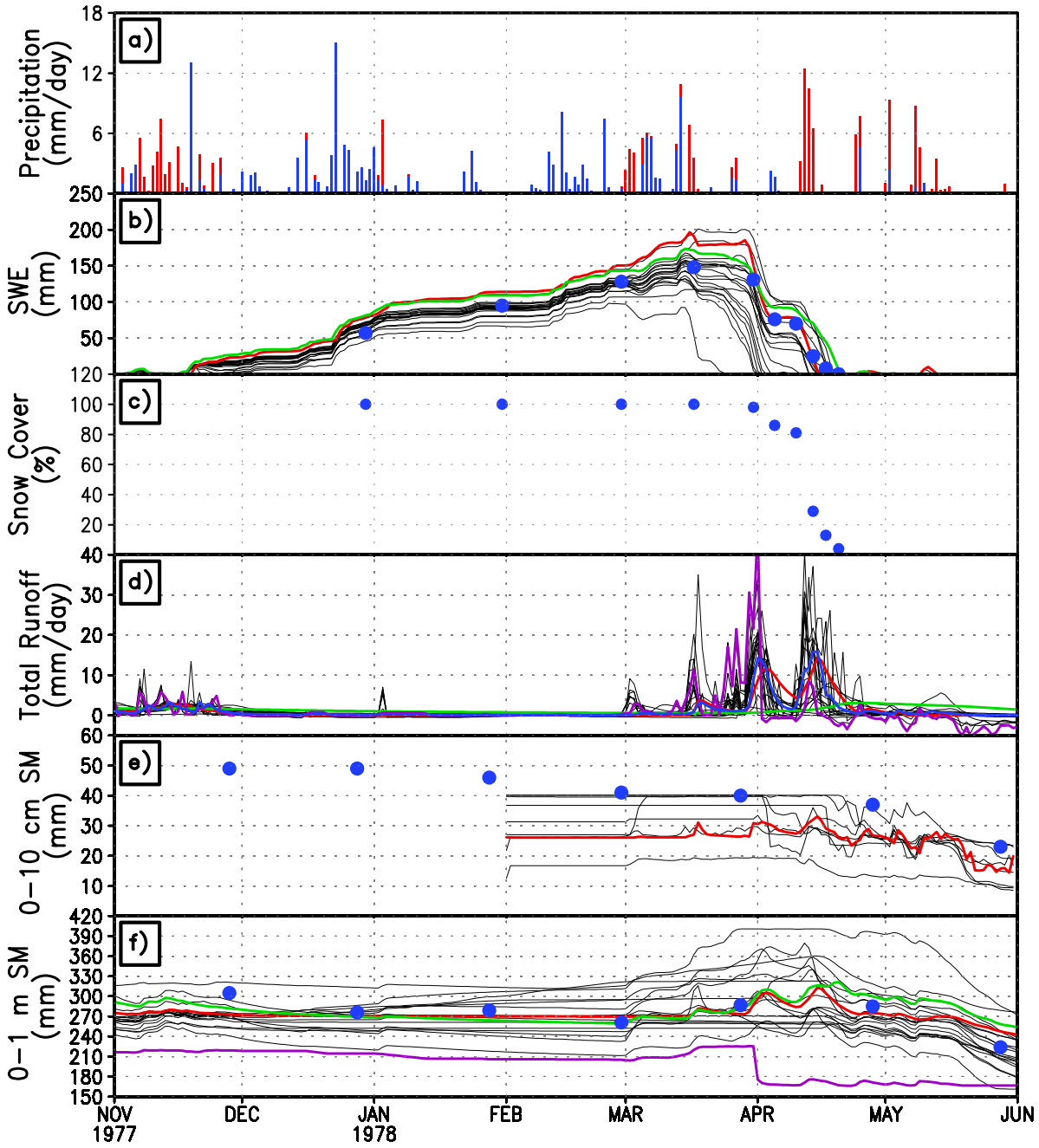

Figure 9 Same as Figure 7, but for the winter of 1977-1978.